Self-assembly and tunable mechanics of reconfigurable colloidal crystals

Kevin L. Kohlstedt[*] and Sharon C. Glotzer[†]

Departments of Chemical Engineering and Materials Science & Engineering, University of Michigan, Ann Arbor, Michigan 48109, USA

(Received 18 April 2012; published 13 March 2013)

We investigate the self-assembly of crystals from reconfigurable colloidal building blocks. The building blocks possess the unique ability, inspired by recent experiments, to continuously alter their shape before, during, and after assembly. Using molecular simulations, we report the assembly of a reconfigurable degenerate crystal containing a fractionally filled kagome sublattice. We show that this degenerate crystal differs from, and assembles more easily than, its counterpart known for rigid dimers. We further report that the reconfigurable crystal has unique mechanical properties under shear strain compared to a crystal comprised of rigid building blocks. We find that even a small amount of reconfigurability in an assembly of otherwise rigid building blocks can greatly affect mechanical properties.

DOI: 10.1103/PhysRevE.87.032305 PACS number(s): 82.70.Dd, 68.65.−k, 36.40.Mr, 64.75.Xc

I. INTRODUCTION

Colloidal building blocks of a variety of shapes, sizes, and interaction patchiness form a rich array of novel phases through self-assembly [1–4]. With few recent exceptions [5,6], in nearly all reported cases of colloidal or nanoparticle self-assembly the building blocks comprising the assembly have a static shape. Recent advances in synthesis have made possible new "reconfigurable building blocks" able to toggle among multiple shapes [5,7] or assemblies [8]. Examples include lock-and-key colloids [9], biphasic microstructures [10], and tunable effective interactions [3,7]. Colloidal building blocks that can reconfigure have an intrinsic dynamism that allow for changes in their shape or interparticle interaction, creating exciting possibilities for assembling a new class of colloidal matter. In particular, shape reconfiguration at the building-block level creates the potential for the assembly of complex structures not otherwise attainable due to kinetic or other reasons [5,11–14]. Furthermore, matter formed from shape-changing building blocks should respond differently to external forces than matter formed from static building blocks. Assemblies of colloidal building blocks with the ability to shape change is not understood but has promise for a wide variety of physical systems such as on-demand sensing [15] and tunable optical properties [16].

In this article, we investigate via computer simulation the self-assembly and mechanical properties of colloidal crystals formed from reconfigurable building blocks. Our building blocks are inspired by, and modeled loosely on, an exciting new type of colloid recently fabricated by Pine and coworkers [9], wherein dimpled "locks" are bound via depletion interactions to colloidal "keys" and freely rotate about the key particle. Here we investigate the planar assembly of already-bound, reconfigurable "two-lock" clusters and determine the effect that local shape reconfiguration has on the phase behavior and mechanical properties of the assembled structures as compared to crystals formed from their rigid counterparts. These relatively simple two-lock clusters are just one example of reconfigurable building blocks that could conceivably be fabricated; other examples include magnetic interactions [17]. We report the assembly of a degenerate crystal (DC) reminiscent of that formed from rigid dimers [18] but distinct due to the formation of sublattices. Degenerate crystals having crystalline order at the monomer level have been observed for rigid, anisotropic structures, e.g., a monolayer tiling of rhombs [19], hard spherical dimers [20,21], or hard polyhedral dimers [22]. The DC we report is unique in that the lattice former has additional degrees of freedom (lock-key bond d_{KL}, lock-key angle ϕ) giving a more complex DC than that previously observed. Finally, we show that the DC formed from reconfigurable two-lock clusters under shear strain has unique mechanical properties compared to rigid colloidal dimers due to alignment of the cluster axes. While shear alignment is commonly observed with either flexible molecules such as wormlike micelles and polymer systems or with hard anisotropic colloids, microfilaments, and other liquid crystalline molecules [23,24], the system considered here is novel in its ability to have aspects of *both* types, i.e., alignment due to internal degrees of freedom while having well-defined orientational order. Due to this reorientation ability, we find even a small minority (10%) of reconfigurable building blocks doped into a DC composed of rigid ones gives qualitatively different bulk properties.

II. MODEL

We construct our model building blocks using spheres bonded together as shown in Fig. 1. The building blocks can behave like linear dimers (in the limit of large lock sizes) but can also reconfigure into nonlinear geometries behaving like colloidal "molecules." The colloids we consider differ from previous models [18,25] in two important respects. First, the geometry differs, generalized here for overlapping spheres with arbitrary size ratio. Second, the interaction between clusters is tunable by effective interactions such as depletion forces, with assembly interactions characterized for lock-and-key geometries [26]. Each cluster consists of a central key (K) of diameter D_K bonded to two locks (L) of diameter D_L. Due to the dimple of the locks [27], we consider bond lengths of $d_{KL} \leqslant (D_K + D_L)/2$. We model the interactions

[*]Current address: Department of Chemistry, Northwestern University, Evanston, IL 60208.

[†]Corresponding author: sglotzer@umich.edu

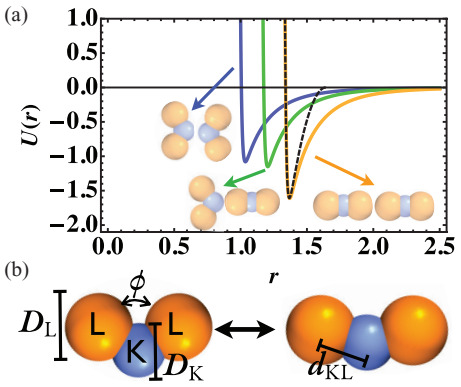

FIG. 1. (Color online) The short-range attractive potential models the depletion interaction among K-K, K-L, and L-L (a). The potential minima (arrows show configuration of minima) are shifted away from the surface by $0.02D_K$ due to the Debye screening and have width $<D_K$. We show a model Asakura-Oosawa potential (dashed) of width $D_K/10$ for reference. The satellite movements are shown for a radius ratio of $\alpha \equiv D_K/D_L = 0.75$ and an key-lock bond distance of $d_{KL} = 0.7$ (b).

between the colloids as

$$U^{mn}(r) = \sum_{i,j} U_R^{mn}(r_{ij}) + \sum_{i,j} U_A^{mn}(r_{ij}) \qquad (1)$$

with a repulsive term $U_R^{mn}(r_{ij})$ derived from the charged double layer and an attractive term that models a short-range attraction $U_A^{mn}(r_{ij})$ between each m-n pair of colloids, where K-K, K-L, and L-L are the three types of interactions in our system. The potentials and parameter values are summarized in Table SI of the Supplemental Materials [28]. The attractive portion of the potential $U_A^{mn}(r_{ij})$ is modeled as a short-range surface potential where a $U \sim 1/r^6$ interaction is shifted by $\Delta^{mn} = \sigma^{mn} - \sigma$. The attractive well width for each m-n pair is always within a distance of σ^{mn} such that all the energetics occur between nearest-neighbor contacts, which leads to attractions between constituent lock particles differentiating them from flexible chains [29,30]. We express all quantities as dimensionless quantities, namely distance $r = \bar{r}/D_K$, time $\tau = \bar{t}/\sqrt{D_K^2 m_K/k_B T}$, pressure $P = \bar{P} D_K^3/k_B T$, and energy $U = \bar{U}/k_B T$. We take the mass of the spheres to be $m_K = m_L = 1$. The bonded locks are able to freely rotate in the plane between angles $\phi_i \in (\phi_{\min}, \pi]$ with respect to each other as shown in Fig. 1(b), where $\phi_{\min}$ is dependent on the geometry of the cluster by $\cos\phi_{\min} = 1 - D_L^2/2d_{KL}^2$. We consider the bond to be of zero mass and do not include any lubrication forces due to wetting in the lock cavity. We constrain the bond distance using the SHAKE algorithm [31].

III. DEGENERATE CRYSTAL

We find the two-lock clusters assemble at high densities into a DC, an example of which is shown in Figs. 2(a) and 2(b). Although the particular geometry of the building block is not a unique DC former, we find as $d_{KL} \to D_K/2 + D_L/2$ and $\alpha \approx 1$ the DC becomes destabilized. In the limit of linear, rigid clusters we recover the model clusters reminiscent of the rigid dumbbells in Ref. [18]. Nevertheless, small-N clusters show a rich phase space, even for geometries previously consistent

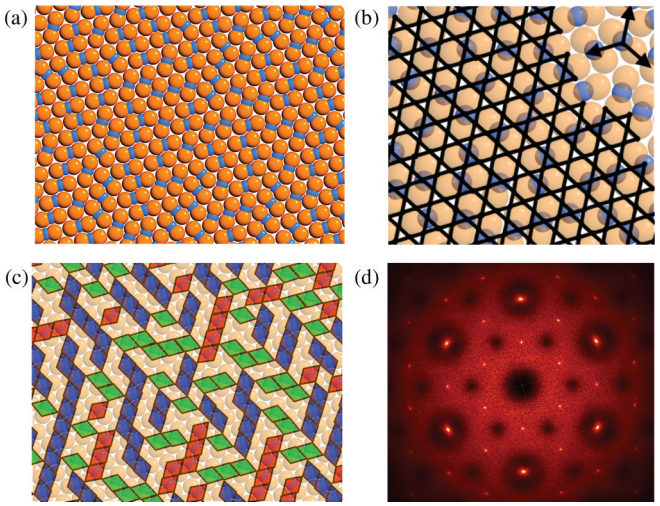

FIG. 2. (Color online) Degenerate crystalline packing of reconfigurable clusters (a) at $P = 11.0$. The vacancies of the kagome sublattice are the interstitials of the DC lattice, while the locks fill the hexagons (b). The RGB rhomb mapping (red is medium gray, green is light gray, and blue is dark gray) is shown overlaid on the clusters (c). The density correlation of the kagome lattice can be visualized with the 2D diffraction pattern of the clusters shows the randomness of the partially filled kagome as well as the sixfold symmetry of the clusters (d).

with DC formation [32]. For this system, we choose a cluster geometry of the keys (blue) and locks (orange) that is both experimentally attainable and consistent with rigid cluster DC formation in order to directly compare with previous results [18]. Namely, the radius ratio and bond length are $\alpha = 0.75$ and $d_{KL} = 0.7$, respectively [see Fig. 1(b)] [9]. The DC is a threefold degenerate lattice with the orientation of the cluster $\langle P(\theta)\rangle$, on average, having an equal probability of being a multiple of $n\pi/3$ with $n = 0,1,2$ (assuming inversion symmetry). Although for large systems $\langle P(\theta)\rangle = n\pi/3$, the local orientational order is correlated due to small energetic gains for like-oriented clusters, stacks of similarly oriented clusters may persist over short distances. We find for our systems an average chain of $\bar{l} = 5.1 \pm 0.3$ or about three clusters. The threefold orientational degeneracy of the building block naturally maps to a tricolored rhomb [33] [Fig. 2(c)], which is similar to a random tiling of molecular rhombs [34]. Because we have a binary system of lock and key particles, we map our system differently by taking the central particle as the center of each rhomb, leading to a tiling that covers exactly half of the cluster space as seen in Fig. 2(c). Further, the mapping limits the tiling to have one and only one 120° angle per neighbor, which is, again, due to the stoichiometry of the two-lock clusters but leads to tilings primarily composed of linear or zigzag rhombs reminiscent of confined colloidal glass formers [35]. The rhombs are used here to visually capture the orientational distribution of clusters in the DC but could also be beneficial in determining the percolation threshold of the lattice or dislocation cage lengths that have been measured for a lattice of dimers [21].

Our DC can be decomposed into two distinguishable, independent sublattices. The locks form a regular hexagonal (triangular) lattice, while the keys lie on a fractionally filled

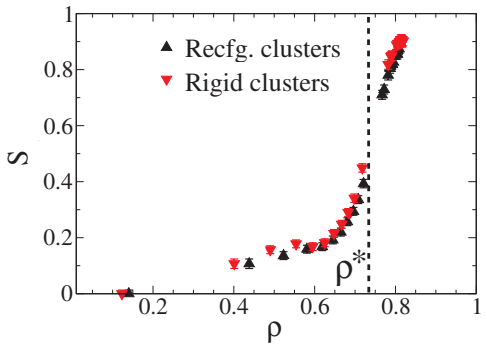

FIG. 3. (Color online) The assembly of the two-lock clusters into the DC for rigid and reconfigurable clusters. Along the direction of increasing packing fraction ρ the order parameter S shows a discontinuous jump at $\rho^* \approx 0.73$ for both reconfigurable (black up-triangles) and rigid clusters [red (gray) down-triangles]. We note that the error bars on S are plotted, but most are smaller than the plot symbols, allowing a detailed comparison between the systems.

kagome lattice (see Fig. 2). We note that the lattices are independent, and if the locks and keys are not permanently bound (i.e., chemically bound) it might be possible for one component to be removed, leaving a single lattice. Due to the stoichiometry of the two-lock clusters the kagome lattice can only be partially (1/6) filled. Local areas of aligned clusters keep an occupancy rule similar to the 2D system of spin-polarized fermions constrained on a kagome lattice [36]. Interestingly, the charge fractionalization on a kagome lattice leads to properties similar to spin ice where no single minimal energy state exists [36]. Although kagome lattices have been long studied in frustrated spin systems [37], colloidal kagome lattices have been of interest lately due to their potential optical properties [3]. Another property of the clusters is that by permuting the local rhomb orientations one can tune the filling fraction of the entire kagome lattice; e.g., a system of locks that make threefold bonds with neighboring keys. Figure 2(c) illustrates the rhomb mapping of a typical configuration at $P \gg 1$ with stacks of like-oriented rhombs forming lines and zigzags. The diffraction pattern of the DC shows the interplay between the periodicity of the kagome lattice (Bragg peaks) with the randomness of the oriented clusters (correlated background noise) in Fig. 2(d).

We expect the assembly propensity to vary with reconfigurability of the building block [14] due to the additional degrees of freedom inherent to the reconfigurable particles. Moreover, reconfigurability can allow cluster shapes incompatible with a DC. In Fig. 3, we compare the self-assembly of the DC from rigid and reconfigurable clusters and compute the degree of order of the DC using an hcp order parameter S [38]. We write S as a similarity metric comparing the locks in the DC to an equivalent hcp lattice using the familiar sixfold bond order parameter q_6 [39]. Namely

$$S = \left\langle q_6^{\mathrm{hex}} q_6^{\mathrm{DC}} \right\rangle, \tag{2}$$

where q_6^k is calculated with k being either the hcp reference lattice or the assembled DC. We consider the order parameter S computed over the first neighbor shell (inclusion of the second neighbor shell in S did not show a qualitative difference) and average over the configuration space. We plot in Fig. 3 the order parameter for both the rigid and reconfigurable clusters with both showing a clear discontinuity in S at a packing fraction $\rho^* \approx 0.73$. At $\rho \approx \rho^*$ the building blocks are highly constrained and the packing of the locks dominates, making the rigid and reconfigurable clusters behave similarly but not identically. We find that our model predicts two effects near ρ^* that are not seen for the rigid case. First, at $\rho \lesssim \rho^*$, the reconfigurable building blocks have less order at the same density due their ability to reconfigure and, thus, have more free volume available to them. Second, at $\rho \gtrsim \rho^*$, the reconfigurable clusters stabilize the DC at lower densities, thereby narrowing the coexistence region. Above ρ^*, the reconfigurable DC lattice has a slightly lower S compared to the rigid case due to the additional degrees of freedom the clusters possess, giving rise to configurations that are not congruent with the kagome lattice. In the infinite pressure limit, of course, both DC lattices become indistinguishable ($S \to 1$). We note that the value of ρ^* for both systems is shifted slightly left compared to the hard rigid dimer system [18] ($\rho^* \approx 0.78$) because the interactions stabilize the lattice at lower densities.

IV. MECHANICAL BEHAVIOR

We investigate the mechanical differences between the assembled crystals of rigid versus reconfigurable building blocks under shear deformation. We are particularly interested in the structural arrangements induced by an applied shear strain [40]. We calculate the global alignment of the clusters for increasing macroscopic strains at a strain rate of $\dot{\varepsilon} = 0.002\,\tau^{-1}$. In Fig. 4, we show the orientational histogram $P(\theta)$ of the clusters for increasing strain ε up to $\varepsilon = 100$. At $\varepsilon = 0$, $P(\theta)$ clearly shows the three degenerate orientations

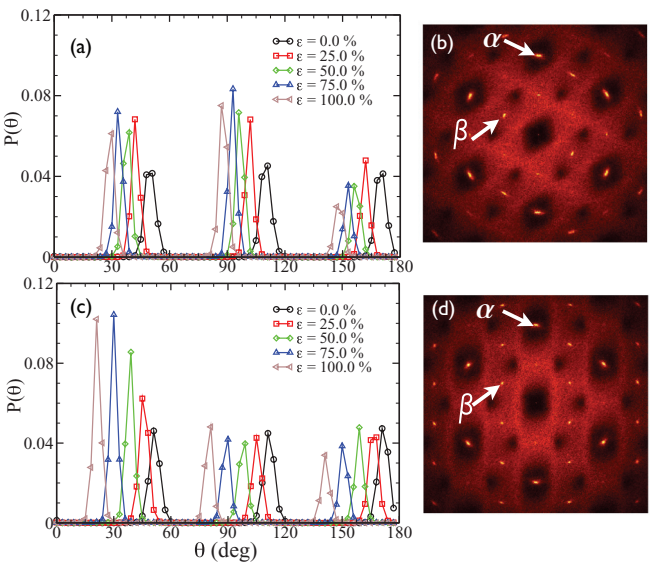

FIG. 4. (Color online) We show the response of a DC at $\rho = 0.86$ (a) composed solely of rigid clusters for increasing strain along the x axis. At $\varepsilon = 75\%$, the diffraction pattern (b) shows some alignment though diffuse nearest-neighbor α peaks compared to the DC [see Fig. 2(d)]. In panels (c) and (d) we show a system containing a 10% mixture of reconfigurable clusters. The diffraction pattern of the centers at $\varepsilon = 75\%$ (d) shows sharp β peaks or orientational stacking.

have equal probability *globally* (as we previously discussed, there are local orientational correlations). To show the role of the reconfigurable clusters in the rearrangement of the DC, we compare the orientation and structure of a DC comprised solely of rigid clusters [Figs. 4(a) and 4(b)] to one having a minority of 10% reconfigurable clusters [Figs. 4(c) and 4(d)]. The first peak of $P(\theta)$ (those clusters that are closely aligned with the shear) for the reconfigurable clusters [Fig. 4(c)] becomes populated at $\varepsilon = 25\%$, while the other orientations deplete and continuously populates until saturated at $\varepsilon = 100\%$. Comparatively, the rigid clusters do not reorient themselves continuously but exhibit a stick-slip-like behavior. We expect that if the reconfigurable clusters do indeed act as slip agents, then the DC crystal should align into like-oriented stacks of clusters. The like-oriented stacks can be readily identified using the 2D structure factor of the keys during shear. As the clusters align into ordered stacks the keys gain positional order through multilayer stacks, which is seen by the emergence of the Bragg peaks labeled as β (Fig. S1 in the Supplemental Materials shows the real-space unit cell) [28]. In Fig. 4(d), we show the β peaks form due to the aligned cluster stacking at $\varepsilon = 75\%$. By comparison, after shearing the rigid DC, the stacks of aligned clusters is not nearly as developed shown by the lack of β Bragg peaks in Fig. 4(b). The aligned stacks formed via shear are the first assemblies to show evidence of aligned phases not predicted to exist in colloidal dimer assemblies [18,25].

In Fig. 4(c), large-scale rearrangements in the cluster axes' orientation due to the applied shear strain is shown by an increase in the population of the first θ peak or from our rhomb mapping—the number of red colored rhombs increases (see Fig. S1 in the Supplemental Materials) [28]. This increase in population levels off at doping amounts near 30%, and, because of this saturation, we infer that the reconfigurable clusters act as slip agents for the rigid clusters. Further, we find for the reconfigurable clusters the bond angle $\phi < 180^\circ$ (Fig. S2 in the Supplemental Materials), providing evidence for a defect mechanism whereby the flexible clusters are able to reorient themselves, allowing the rigid clusters to slip [28].

V. CONCLUSION

We have shown that the self-assembly of a threefold degenerate crystal is robust for these reconfigurable colloidal building blocks. Furthermore, within the DC the key particles lie on a fractionally filled kagome sublattice where the degree of fractionalization is controlled by the randomness of the oriented clusters. The tunability of the DC randomness leads naturally to applications in information theory and cryptography [41], while the mechanical properties of the DC can also be tuned via the reconfigurability of the building block, thereby controlling the time scale of local plastic deformation. We expect assemblies containing reconfigurable building blocks, especially for nonconvex particles, to be more deformable than rigid building blocks due to their ability to locally alter their shape. In order for clusters to change orientations in the DC, reorientation must occur around local defects. A model where the locks and keys are not permanently bonded to each other and where the bond angle is not fixed in two dimensions will be required to get access to an experimentally realizable mechanism. The reconfigurability of the locks allows the orientation of the clusters to occur with a pivot move shown in Fig. 1(b). We note that this could be the first colloidal system to have a rearrangement mechanism that does not require such a restricted dislocation mechanism for rearrangement [21]. These systems are tractable model systems to understand bulk properties of amorphous or polycrystalline materials [42,43], especially when formed from complex building blocks. Reconfigurable building blocks provide an opportunity for local shape change to produce significant changes on much larger scales. We expect these results could provide a basis for understanding biological reconfigurable processes such as conformation cooperativity in allosteric proteins or mechanical shape change of cells due to microfilament realignment that are well known in biology [44]. An experimental system testing the shear stress of the lock-and-key colloidal assemblies would be expected to show a significant decrease in the shear modulus compared to assemblies of rigid building blocks.

ACKNOWLEDGMENTS

The authors thank David Pine for extensive conversations on the details of the lock-and-key system, and Michael Engel for stimulating discussions and help in the visualization of this system. This work was supported by the US Army Research Office under Grant No. W911NF-10-1-0518. S.C.G. is also supported by the DOD/ASDRE under Award No. N00244-09-1-0062.

[1] K. Miszta *et al.*, Nat. Mater. **10**, 872 (2011).
[2] A. V. Tkachenko, Phys. Rev. Lett. **106**, 255501 (2011).
[3] Q. Chen, S. C. Bae, and S. Granick, Nature **469**, 381 (2011).
[4] S. C. Glotzer and M. J. Solomon, Nat. Mater. **6**, 557 (2007).
[5] Y. G. Zhang, F. Lu, D. van der Lelie, and O. Gang, Phys. Rev. Lett. **107**, 135701 (2011).
[6] J.-W. Yoo and S. Mitragotri, Proc. Natl. Acad. Sci. USA **107**, 11205 (2010).
[7] E. Klavins, IEEE Control Syst. Mag. **27**, 43 (2007).
[8] K. L. Young *et al.*, Proc. Natl. Acad. Sci. USA **109**, 2240 (2012).
[9] S. Sacanna, W. T. M. Irvine, P. M. Chaikin, and D. J. Pine, Nature **464**, 575 (2010).
[10] S. Saha, D. Copic, S. Bhaskar, N. Clay, A. Donini, A. J. Hart, and J. Lahann, Ang. Chem. Ed. **51**, 660 (2012).
[11] O. Gang and Y. G. Zhang, ACS Nano **5**, 8549 (2011).
[12] E. Jankowski and S. C. Glotzer, Soft Matter **8**, 2852 (2012).
[13] T. D. Nguyen and S. C. Glotzer, ACS Nano **4**, 2585 (2010).
[14] T. D. Nguyen, E. Jankowski, and S. C. Glotzer, ACS Nano **5**, 8892 (2011).
[15] J. H. Holtz and S. A. Asher, Nature **389**, 829 (1997).

[16] S. A. Maier, M. L. Brongersma, P. G. Kik, and H. A. Atwater, Phys. Rev. B **65**, 193408 (2002).
[17] S. Sacanna, L. Rossi, and D. J. Pine, J. Am. Chem. Soc. **13**, 6112 (2012).
[18] K. W. Wojciechowski, D. Frenkel, and A. C. Branka, Phys. Rev. Lett. **66**, 3168 (1991); S. H. Lee, S. J. Gerbode, B. S. John, A. K. Wolfgang, F. A. Escobedo, I. Cohen, and C. M. Liddell, J. Mater. Chem. **18**, 4912 (2008).
[19] J. P. Garrahan, A. Stannard, M. O. Blunt, and P. H. Beton, Proc. Natl. Acad. Sci. USA **106**, 15209 (2009); S. Whitelam, I. Tamblyn, P. H. Beton, and J. P. Garrahan, Phys. Rev. Lett. **108**, 035702 (2012).
[20] A. P. Malanoski and P. A. Monson, J. Chem. Phys. **107**, 6899 (1997).
[21] S. J. Gerbode, S. H. Lee, C. M. Liddell, and I. Cohen, Phys. Rev. Lett. **101**, 058302 (2008).
[22] A. Haji-Akbari, M. Engel, and S. C. Glotzer, Phys. Rev. Lett. **107**, 215702 (2011).
[23] M. E. Cates and S. T. Milner, Phys. Rev. Lett. **62**, 1856 (1989).
[24] H. Hahn, J. H. Lee, N. P. Balsara, B. A. Garetz, and H. Watanabe, Macromolecules **34**, 8701 (2001); M. J. Solomon *et al.*, Macromolec. Rapid Commun. **31**, 196 (2010).
[25] C. McBride and C. Vega, J. Chem. Phys. **116**, 1757 (2002); C. Vega, E. P. A. Paras, and P. A. Monson, *ibid.* **96**, 9060 (1992).
[26] F. Jimenez-Angeles, G. Odriozola, and M. Lozada-Cassou, J. Mol. Liq. **164**, 87 (2011).
[27] S. Sacanna, W. T. M. Irvine, L. Rossi, and D. J. Pine, Soft Matter **7**, 1631 (2011).
[28] See Supplemental Material at http://link.aps.org/supplemental/10.1103/PhysRevE.87.032305 for details on the simulation; for the definition of the β Bragg peak; for a typical sheared DC with rhomb tiling; for details on slip mechanism.
[29] J. M. Polson and D. Frenkel, J. Chem. Phys. **109**, 318 (1998).
[30] E. Sanz, C. McBride, and C. Vega, Mol. Phys. **101**, 2241 (2003).
[31] E. Barth, K. Kuczera, B. Leimkuhler, and R. D. Skeel, J. Comput. Chem. **16**, 1192 (1995).
[32] C. Reichhardt and C. J. Reichhardt, Phys. Rev. E **85**, 051401 (2010).
[33] F. Alet, J. L. Jacobsen, G. Misguich, V. Pasquier, F. Mila, and M. Troyer, Phys. Rev. Lett. **94**, 235702 (2005).
[34] M. O. Blunt, J. C. Russell, M. D. Gimenez-Lopez, J. P. Garrahan, X. Lin, M. Schroder, N. R. Champness, and P. H. Beton, Science **322**, 1077 (2008).
[35] Y. Shokef and T. C. Lubensky, Phys. Rev. Lett. **102**, 048303 (2009).
[36] A. Ruegg and G. A. Fiete, Phys. Rev. B **83**, 165118 (2011).
[37] E. Runge and P. Fulde, Phys. Rev. B **70**, 245113 (2004).
[38] A. S. Keys, C. R. Iacovella, and S. C. Glotzer, Ann. Rev. Condensed Matter Phys. **2**, 263 (2011).
[39] B. I. Halperin and D. R. Nelson, Phys. Rev. Lett. **41**, 121 (1978).
[40] E. J. Stancik, A. L. Hawkinson, and G. G. Fuller, J. Rheol. **48**, 159 (2004).
[41] A. Hache, M. Malik, M. Diem, L. Tkeshelashvili, and K. Busch, Photon. Nanostruct. **5**, 29 (2007).
[42] P. Schall, D. A. Weitz, and F. Spaepen, Science **318**, 1895 (2007).
[43] Y. F. Shi and M. L. Falk, Phys. Rev. Lett. **95**, 095502 (2005).
[44] G. B. Blanchard, A. J. Kabla, N. L. Schultz, L. C. Butler, B. Sanson, N. Gorfinkiel, L. Mahadevan, R. J. Adams, Nat. Methods **6**, 458 (2009).